RODOS-DIPCOT Model Description and Evaluation

RODOS(RA2)-TN(09)-01

Spyros Andronopoulos, Efstratios Davakis

Environmental Research Laboratory, Institute of Nuclear Technology and Radiation Protection, National Centre for Scientific Research "Demokritos"

15310 Aghia Paraskevi, Greece

Email: sandron@ipta.demokritos.gr

John G. Bartzis

University of Western Macedonia, Department of Mechanical Engineering

Bakola & Sialvera Str., 50100, Kozani, Greece

Email: bartzis@uowm.gr

Final, 31 July 2009

Management Summary

DIPCOT (DISPersion over COmplex Terrain) is an atmospheric dispersion model, which simulates the dispersion of air pollutants over complex terrain. It is a Lagrangian puff / particle model in which the mass of the pollutants is distributed to a certain number of fictitious puffs or particles that are displaced in the computational domain according to the wind velocity to which a random component is added to account for turbulent diffusion. The knowledge of the spatial and temporal distribution of the particles allows the calculation of the pollutants air concentration of at specified locations and times.

DIPCOT has been integrated in RODOS and runs both in the automatic (diagnosis and prognosis) and interactive (prognosis) modes. This report describes the physics for the puffs / particles displacement, turbulence parameterisation, calculation of concentration, dry and wet deposition and gamma radiation dose rate calculation. Finally the report includes performance evaluation studies of the model against well known field experimental data, using established methodologies.

Contents

1 Introduction

The DIPCOT model (**DI**s**P**ersion over **CO**mplex **T**errain) is a computer code, which simulates the dispersion of air pollutants over complex terrain. The model has the ability to simulate atmospheric dispersion in both homogeneous and inhomogeneous conditions based on a Lagrangian particle model scheme. The mass of the pollutants is distributed to a certain number of fictitious puffs or particles that are displaced in the computational domain according to the wind velocity to which a random component is added to account for turbulent diffusion. The knowledge of the spatial and temporal distribution of the particles allows the calculation of the pollutants air concentration of at specified locations and times.

DIPCOT uses topographical and meteorological information given on a 3-D grid and is capable of simulating dispersion of multiple pollutants from multiple point sources. In the case of buoyant point sources the model performs plume rise calculations. If applicable, the code also calculates dry and wet deposition on the ground and, in case of radioactive pollutants, the gamma radiation dose rates. Three types of input data, concerning the source characteristics, topography and meteorology are necessary for the simulations. The emission characteristics (i.e., source location, release height, emission rate, stack diameter, gas exit velocity and temperature) are provided by the RODOS Source Term Module (or are calculated from the data provided by it), while 'gridded' topographical and meteorological information are provided by the RODOS Meteorological Pre-Processor (RMPP). DIPCOT uses 3-dimensional fields for the wind velocity, temperature, and pressure and 2-dimensional fields for topography, ground roughness, mixing layer height, friction velocity, convective velocity, category of atmospheric stability, precipitation intensity and Monin-Obukhov length. The model calculates instantaneous air concentrations, time-integrated air concentrations, dry and wet deposition rates and deposition of pollutants, gamma radiation dose rates and time-integrated dose (cloud and ground) at the locations of the RODOS dispersion grid and at locations of detectors.

This document describes the physics of the atmospheric dispersion and gamma radiation dose rates models included in RODOS-DIPCOT. The RODOS-DIPCOT is an adapted version of the stand-alone DIPCOT code, previously developed in the Environmental Research Laboratory. The document includes also model performance evaluation studies against real-scale experimental data.

2 The dispersion model description

2.1 The puffs/particles displacement model

The DIPCOT model simulates the atmospheric dispersion of passive pollutants (i.e., pollutants that do not influence the underlying wind velocity field, due to, e.g., different density), using a Lagrangian puff/particle methodology based on Langevin equation for the determination of random velocity increments, in order to take into account turbulent velocity fluctuations.

The particles are released in the atmosphere and the particle trajectories are calculated according to the following equation:

$$x_i^{n+1} = x_i^{n} + \left(\overline{u_i} + u_i'\right)\Delta t \tag{1}$$

in which n is the time-step index, i is the Cartesian direction index (i = 1, 2, or 3 for the 3 directions), $\overline{u_i}$ is the mean wind velocity component in direction i, and u_i' represents the turbulent velocity fluctuations. Assuming that a) the velocity and the position of each particle evolve as a Markov process and b) there is mutual independence of the three velocity components, u_i' is estimated using the one-dimensional Langevin equation (Thomson, 1987):

$$du_i' = a_i dt + b_i dW_i(t) \tag{2}$$

where du_i' is the change in turbulence velocity over time interval dt. The parameters α_i and b_i (also known as "drift" and "diffusion" terms respectively) are, in general, functions of time, space and velocity. It should be noticed that this approach assumes that the particles' accelerations are uncorrelated, since they can be described by a white noise process, and that particle velocities are correlated up to the Lagrangian time scale T_{Lui}, which is characteristic of the energy containing eddies. This is a good assumption (Luhar and Rao 1993) since, "in high Reynolds number flows, the accelerations of a particle at two successive time steps are practically correlated for times only of the order Kolmogorov's time scale $\tau_n = \mathrm{Re}^{1/2} T_{Lui}$", which is characteristic of the scales on which viscous processes convert turbulent kinetic energy into heat. "Therefore, particle accelerations can be assumed to be uncorrelated for time steps which lie in the inertial subrange i.e. $\tau_n << \Delta t << T_{Lui}$ (Monin and Yaglom, 1975, §21.5)".

Equation (2) is able to simulate atmospheric dispersion in several conditions, with appropriate choice of the two coefficients. The drift term α_i is determined through the consistency between the Lagrangian and the Eulerian statistics. In order to estimate the value of α_i we assume that if the Eulerian statistics are known, they should be considered as a restriction on the form of the Langevin equation (Thomson 1987, Wilson and Sawford 1996). This constraint is expressed through Fokker-Plank equation, which is the Eulerian analogue of Langevin equation:

$$\frac{\partial P_a}{\partial t} + \frac{\partial (u_i' P_a)}{\partial x_i} = -\frac{\partial (\alpha_i P_\alpha)}{\partial u_i'} + \frac{1}{2}\frac{\partial (b_i^2 P_a)}{\partial u_i'^2}$$

where P_a is Eulerian velocity probability density function (pdf), which is considered known. The above equation can now be solved for each component, considering also stationary turbulence ($\partial P_a / \partial t = 0$) and that at a small time interval Δt the velocity of a particle is independent of its position ($\partial u_i' / \partial x_i = 0$):

$$a_i = \left[\frac{\partial}{\partial u_i'} \left(\frac{1}{2} b_i^2 P_a \right) + \phi_i \right] / P_a \quad (3)$$

where $\partial \phi_i / \partial u_i' = -u_i' \partial P_a / \partial x_i$ (Luhar and Britter 1989). Here, P_a is the Eulerian velocity probability density function (pdf). The diffusion term b_i can be obtained through the consistency with the Kolmogorov's similarity theory, by comparing the estimated by (2) Lagrangian velocity structure function with that obtained from Kolmogorov's theory (Luhar and Britter 1989):

$$b_i = \left(2\sigma_{ui}^2 / T_{Lui} \right)^{1/2} \quad (4)$$

where σ_{ui} is the standard deviation of wind fluctuations and T_{Lu}i is the Lagrangian time scale. The model can be applied to different meteorological conditions, according to the selection of the appropriate pdf.

In the convective boundary layer, for unstable conditions, turbulence in the vertical direction can be considered as inhomogeneous and skewed. The *pdf* can be 'constructed' from two Gaussian distributions (Baerentsen and Berkowicz, 1984):

$$P_a(u_3, x_3) = A(x_3) P_A(u_3, x_3) + B(x_3) P_B(u_3, x_3)$$

where

$$P_A = 1/\sqrt{2\pi}\sigma_A \exp\left[-0.5 \left(\left(u_3' - \overline{u_A} \right) / \sigma_A \right)^2 \right]$$

and

$$P_B = 1/\sqrt{2\pi}\sigma_B \exp\left[-0.5 \left(\left(u_3' + \overline{u_B} \right) / \sigma_B \right)^2 \right]$$

are the Gaussian distributions with standard deviations σ_A and σ_B and mean values $\overline{u_A}$ and $\overline{u_B}$ respectively. Assuming that the Eulerian moments of the vertical velocity fluctuations $\left(\overline{u_3'} = 0, \sigma_3^2 (\equiv \overline{u_3'^2}), \overline{u'^3} \right)$ are known up to the third one and that σ_A, σ_B equal $\overline{u_A}, \overline{u_B}$, respectively, all the unknown variables of equation (5) can be determined by the relation:

$$\int_{-\infty}^{\infty} u_3'^m P_{a3} du_3' = \overline{u_3'^m}$$

in which, m=0,1,2,3. Solving the above system with the closure relations explicit solutions of the six unknown parameters are obtained (Luhar and Britter, 1989):

$$\overline{u_B} = \frac{\sqrt{(\overline{u_3'^3})^2 + 8\sigma_{u3}^2} - \overline{u_3'^3}}{4\sigma_{u3}^2}$$

$$\overline{u_A} = \frac{\sigma_{u3}^2}{2\overline{u_B}}$$

$$A = \frac{\overline{u_B}}{\overline{u_A} + \overline{u_B}}$$

$$B = \frac{\overline{u_A}}{\overline{u_A} + \overline{u_B}}$$

and $\overline{u_3'^3} = S_K \sigma_{u3}^3$, where S_K is the skewness of the Eulerian velocity. The term α_3 can now be determined using equation 3:

$$\alpha_3 = \frac{-\frac{\sigma_3^2}{T_{Lu3}} Q_w + \phi_3}{P_\alpha}$$

with

$$Q_3 = \frac{A(u_3' - \overline{u_A})}{\overline{u_A}^2} P_A + \frac{B(u_3' + \overline{u_B})}{\overline{u_B}^2} P_B$$

$$\phi_3 = -\frac{1}{2}\left(A\frac{\partial \overline{u_A}}{\partial x_3} + \overline{u_A}\frac{\partial A}{\partial x_3}\right) erf\left(\frac{u_3' - \overline{u_A}}{\sqrt{2}\sigma_A}\right) +$$

$$\sigma_A\left\{ A\frac{\partial \sigma_A}{\partial x_3}\left(1 + \frac{u_3'(u_3' - \overline{u_A})}{\sigma_A^2}\right) + \sigma_A\frac{\partial A}{\partial x_3} + \frac{A u_3'}{\sigma_A}\frac{\partial \overline{u_A}}{\partial x_3}\right\} P_A$$

$$+\frac{1}{2}\left(B\frac{\partial \overline{u_B}}{\partial x_3} + \overline{u_B}\frac{\partial B}{\partial x_3}\right) erf\left(\frac{u_3' + \overline{u_B}}{\sqrt{2}\sigma_B}\right) +$$

$$\sigma_B\left\{ B\frac{\partial \sigma_B}{\partial x_3}\left(1 + \frac{u_3'(u_3' + \overline{u_B})}{\sigma_B^2}\right) + \sigma_B\frac{\partial B}{\partial x_3} - \frac{B u_3'}{\sigma_B}\frac{\partial \overline{u_B}}{\partial x_3}\right\} P_B$$

Under stable conditions the vertical dispersion is treated presuming inhomogeneous Gaussian turbulence. The Eulerian pdf is now $P_\alpha = \sqrt{2\pi}\sigma_{u3}\exp\left(-u'^2/2\sigma_{u3}^2\right)$. Using equation the equation for the determination of Φ_3 ($\partial\phi_i/\partial u_i' = -u_i'\partial P_a/\partial x_i$) we find that:

$$\phi_3 = \frac{1}{2} P_a \frac{\partial \sigma_{u3}^2}{\partial x_3}\left[1 + \frac{u_3'^2}{\sigma_{u3}^2}\right]$$

From equation (3) and (4) it can be obtained that:

$$\alpha_3 = -\frac{u_3'}{T_{Lu3}} + \frac{1}{2}\left(\frac{u_3'^2}{\sigma_{u3}^2} + 1\right)\frac{\partial \sigma_{u3}^2}{\partial x_3}$$

For the horizontal dispersion, homogeneous isotropic Gaussian turbulence is considered under all the stability conditions. The Eulerian probability density function for the two horizontal velocity components is $P_\alpha = \frac{1}{\sqrt{2\pi}\sigma_{ui}}\exp\left(-\frac{u_i'^2}{2\sigma_{ui}^2}\right)$. In this case $\phi = 0$ (Borgas and Sawford, 1994). Using again equations (3) and (4) we find that:

$$\alpha_1 = -\frac{1}{T_{Lu1}}u_1' \text{ and } \alpha_2 = -\frac{1}{T_{Lu2}}u_2'$$

It should be noticed that in case of convective conditions the particles are perfectly

reflected at the boundaries (ground and top of the mixing layer), while under stable conditions only ground level reflection is considered. The time step for the particle's displacement is based on the vertical dispersion parameterisation (Thomson 1987):

$$\Delta t = \min\left(0.05T_{Lu3}, 0.1\sigma_{u3}/\left|\alpha_3\right|, \sigma_{u3}/\left|u_3'\partial\sigma_{u3}/\partial x_3\right|\right) \qquad \text{if } L < 0$$

$$\Delta t = 0.05T_{Lu3} \qquad \text{if } L \geq 0$$

in which, L is the Monin-Obukhov length.

2.2 The concentration calculations model

Following the displacement of all particles a kernel density estimator is employed to compute the concentrations. In the Lagrangian atmospheric dispersion models two methods are used for the estimation of concentration at a given location (Uliasz, 1993): the box-counting method and the density kernel estimation method. Both methods have been implemented in RODOS-DIPCOT. They are selected by the user through the variable `IEDIT` in the RODOS Assign Editor.

2.2.1 Method 1

In the box-counting method (`IEDIT = 1`) the concentration in a receptor (x,y,z) at time t is computed by counting the number of the particles contained at time t in an imaginary "box" or cell of volume $\Delta x\,\Delta y\,\Delta z$ surrounding the location of interest.

$$c(x,y,z) = \frac{\sum_{i=1}^{N} Q_i}{\Delta x\,\Delta y\,\Delta z} \tag{5}$$

where N is the number of particles inside the cell of volume $\Delta x\,\Delta y\,\Delta z$, and Q_i is the load (e.g., mass, radioactivity) assigned to particle i. In order to reproduce a "smooth" concentration distribution with the box-counting method a large number of particles should be used in the calculations. Moreover the cells dimensions should be carefully selected for each application (Uliaz, 1993, Davakis et al., 2003). In RODOS-DIPCOT the cells horizontally coincide with those of the RODOS grid, while their vertical dimension (Δz) is set equal to 50 m. If the number of released particles is adequate then the box-counting method is the method most closely and accurately representing the actual pollutants dispersion in complex topographies.

2.2.2 Method 2

To overcome the requirement of large number of particles, the kernel estimation method proposed by Yamada and Bunker (1988) is also implemented in RODOS-DIPCOT (Davakis et al., 2003) and is selected by setting `IEDIT = 0`. It is assumed that each particle represents the centre of a puff where the concentration is distributed in a Gaussian manner in 3 directions. In the general case, the concentration at the point (x,y,z) is calculated by summing the contribution from all the particles-puffs present in the computational domain:

$$c(x,y,z) = \frac{1}{(2\pi)^{3/2}} \sum_{i=1}^{N} \frac{Q_i}{\sigma_{xi}\,\sigma_{yi}\,\sigma_{zi}} \exp\left[-\frac{1}{2}\frac{(x_i - x)^2}{\sigma_{xi}^2}\right] \exp\left[-\frac{1}{2}\frac{(y_i - y)^2}{\sigma_{yi}^2}\right] \left\{\exp\left[-\frac{1}{2}\frac{(z_i - z)^2}{\sigma_{zi}^2}\right] + \exp\left[-\frac{1}{2}\frac{(z_i + z - 2z_g)^2}{\sigma_{zi}^2}\right]\right\} \quad (6)$$

where: (x,y,z) are the coordinates of the point where the concentration is estimated, (x_i,y_i,z_i) are the coordinates of the centre of puff i, $(\sigma_{hi}, \sigma_{zi})$ are the standard deviations of the i-particle position in the horizontal and vertical directions respectively (defining the Gaussian concentration distribution in puff i), Q_i is the "load" (e.g., mass, radioactivity) of puff i, z_g is the ground height at (x, y).

In the RODOS-DIPCOT the concentration is calculated by equation (6) at the RODOS-grid points (centres of the RODOS-grid cells) at a height z = 1 m.

The variances in the three directions x, y and z are determined as the time integration of the velocity variances, based on the Taylor's (1921) homogeneous diffusion theory. The variances of particle i are obtained from:

$$\sigma_{xi}^2 = 2\sigma_{u1}^2 \int_0^t \int_0^\zeta R(\zeta)\,d\zeta\,dt = 2\sigma_{u1}^2 T_{Lu1}\left[t + T_{Lu1}\exp\left(-\frac{t}{T_{Lu1}}\right) - T_{Lu1}\right] \quad (6a)$$

$$\sigma_{yi}^2 = 2\sigma_{u2}^2 \int_0^t \int_0^\zeta R(\zeta)\,d\zeta\,dt = 2\sigma_{u2}^2 T_{Lu2}\left[t + T_{Lu2}\exp\left(-\frac{t}{T_{Lu2}}\right) - T_{Lu2}\right] \quad (6b)$$

$$\sigma_{zi}^2 = 2\sigma_{u3}^2 \int_0^t \int_0^\zeta R(\zeta)\,d\zeta\,dt = 2\sigma_{u3}^2 T_{Lu3}\left[t + T_{Lu3}\exp\left(-\frac{t}{T_{Lu3}}\right) - T_{Lu3}\right] \quad (6c)$$

where σ_{u1}^2, σ_{u2}^2, σ_{u3}^2 are the velocity variances in x, y and z-directions respectively, $R(\zeta) = \exp\left(-\zeta / T_{Lu1,2,3}\right)$ is the autocorrelation function of the Lagrangian velocity and T_{Lu1}, T_{Lu2}, T_{Lu3} are the Lagrangian time scales in x, y and z-directions respectively. Although turbulence is generally non-homogeneous, we assume that the theory is applicable over short periods of times, as the time step we use for the particles' displacement is very small compared to the total time of displacement. The variances of the Gaussian distribution represent the characteristic length of influence (bandwidth) for each particle.

In the RODOS-DIPCOT, following the calculations (6a – c) the variances in the horizontal directions are set equal to each other:

$$\sigma_{xi} = \sigma_{yi} = \max\left(\sigma_{xi}, \sigma_{yi}\right)$$

To reduce the required computational time for calculating concentrations by equation (6), a maximum "radius of influence" R_{max} is defined for each puff, so that not all puffs are taken into account in the sum of equation (6), but only those for which the point (x,y,z) is inside their radius of influence. The R_{max} is defined as the distance from the puff's centre where the concentration drops to a certain fraction of the puff's centre concentration. This fraction is set by the user through the variable `CRELMIN` of the RODOS Assign Editor. The default value is `CRELMIN` = 0.001.

$$R_{\max} = \sigma_{xi}\left[-2\ln\left(C_{RELMIN}\right)\right]^{1/2}$$

The same method is used in RIMPUFF model (Thykier-Nielsen et al., 1998). There it is calculated that by taking CRELMIN = 0.001, most of the puff's load (99.98%) is included in $R_{\max}$.

2.3 Parameterisation of turbulence statistics

The dispersion parameters (wind velocity variance and Lagrangian time scale) are estimated from empirical relations depending on atmospheric stability.

In unstable conditions, the standard deviation of wind fluctuations is determined from the equations proposed by Gryning et al. (1987) and Holtslag and Moeng (1991):

$$\sigma_{u1} = \sigma_{u2} = u_*\left[0.35\left(-h/\kappa L\right)^{2/3} + \left(2 - z/h\right)\right]^{1/2}$$
$$\sigma_{u3}^3 = \left[1.6u_*^2\left(1 - z/h\right)\right]^{3/2} + 1.2w_*^3\left(z/h\right)\left(1 - 0.9z/h\right)^{3/2}$$

where z is the height above ground, u_* is friction velocity, w_* is the convective velocity, h is the mixing layer height and L is the Monin – Obukhov length.

Under stable conditions the variance of velocity fluctuations is determined according to Hanna (1982):

$$\sigma_{u1} = \sigma_{u2} = 2u_*\left(1 - z/h\right)$$
$$\sigma_{u3} = 1.3u_*\left(1 - z/h\right)$$

In neutral conditions the formulations proposed by Hanna (1982) are adopted,

$$\sigma_{u1} = \sigma_{u2} = 2u_*\exp\left(-3f_C z/u_*\right)$$
$$\sigma_{u3} = 1.3u_*\exp\left(-2f_C z/u_*\right)$$

in which, f_C is the Coriolis parameter.

Finally minimum values of 0.1 and 0.05 are imposed for $\sigma_{u1,2}$ and σ_{u3} respectively.

The Lagrangian time scale is given by the following formulas:

For unstable conditions (Hanna, 1982):

$$T_{L1} = T_{L2} = 0.15h/\sigma_{u1}$$

$$T_{L3} = 0.1\frac{z}{\sigma_{u3}\left[0.55 + 0.38\left(z - z_0\right)/L\right]} \text{ for } z < 0.1h \text{ and } z\text{-}z_o > \text{-}L$$

$$T_{L3} = 0.59\frac{z}{\sigma_{u3}} \text{ for } z < 0.1h \text{ and } z\text{-}z_o < \text{-}L$$

$$T_{L3} = 0.15\frac{z}{\sigma_{u3}}\left[1 - \exp\left(-\frac{5z}{h}\right)\right] \text{ for } z \geq 0.1h$$

where z_0 is the roughness length.

For stable conditions:

$$T_{L3} = 0.1\frac{h}{\sigma_{u3}}\left(\frac{z}{h}\right)^{0.8}$$

$$T_{L1} = T_{L2} = 7.5T_{L3}$$

For neutral conditions:

$$T_{L3} = \frac{0.375\,z/\sigma_{u3}}{1+15\,f_C z/u_*}$$

$$T_{L1} = T_{L2} = 3T_{L3}$$

The above relations for stable and neutral conditions are modifications of those suggested by Hanna (1982).

The skewness of the Eulerian velocity S_K at the stable conditions is equal to 0, while in convective conditions is given by the relation proposed by Weil (1990):

$$S_K = \overline{u_3'^3}/\sigma_{u3}^3 = 0.84(z/h)(1-z/h)w_*^3/\sigma_{u3}^3$$

2.4 Plume rise calculations

If buoyant point sources are considered, where the gas temperature is greater than air's, plume rise calculations are performed, following the algorithm proposed by Hurley and Physic (1993). Thus, after the release, each particle is displaced in the vertical direction, until it reaches the final plume height, using the equations that govern the rise of a bent-over plume (Briggs1975). It is assumed that the plume rises adiabatically, and that the gas is cooling only due the expansion. The three basic equations for a bent over plume are:

$$\frac{dF}{dt} = -N^2 M, \quad \frac{dM}{dt} = F, \quad \frac{dZ_{PL}}{dt} = w_{PL} \tag{7}$$

where F is the plume buoyancy, $N^2 = g/T_a(d\theta/dz)$ is the Brunt Väissälä frequency, $M = w_{PL}U_h\beta_R^2 Z_{PL}^2$ is the momentum, Z_{PL} is the rise height of the plume above the source, w_{PL} is the rise velocity, g is gravity acceleration, T_α is the ambient temperature of air (K), θ is the potential temperature (K), U_h is the ambient horizontal wind velocity, β_R is a constant which is 0.5 for stable and neutral conditions ($L > 0$) and 0.6, 0.65, 0.7 and 0.75 for convective conditions (L > 0 and stability category D, C, B and A respectively). The initial values at the release point are:

$$M_o = w_o^2 r_s^2\, T_\alpha/T_s$$

$$F_o = g w_o r_s^2 (1 - T_a/T_s)$$

$$r_o = r_s\left[T_\alpha w_o/(T_o U_h)\right]^{1/2}$$

$$Z_o = r_o/\beta_R$$

where w_o is the gas exit velocity from the stack, T_s is the gas exit temperature (K) and r_s is the stack radius.

In the case of convective and neutral conditions the potential temperature gradient $d\theta/dz \le 0$. Hence in order to produce real solutions from the system of equations (7) we must assume that N^2=0. Under this assumption, equations (7) have an analytical solution, which provides the rise above the stack for small time intervals.

$$Z_{PL}^{n+1} = \left\{ \left(Z_{PL}^{n}\right)^3 + \frac{3}{U_h \beta_R^2}\left[M_o\left(t_{n+1} - t_n\right) + \frac{F_o}{2}\left(t_{n+1}^2 - t_n^2\right)\right]\right\}^{1/3}$$

This solution enables the use of the available meteorological information at each level of rise. It is assumed that each particle reaches the effective stack height (i.e. the final height of the rise) when the plume dissipation rate $E_{PL} = 1.5 w_{PL}^3 / Z_{PL}$ becomes equal to the ambient dissipation rate $E_\alpha = 0.6 w_*^3 / h$.

In the case of stable conditions the simultaneous ordinary differential equations (7) are solved using a 4th order Runge-Kutta scheme, using time step equal to $\Delta t/5$, which also enables the use of time and height varying meteorological parameters. The rise is terminated when the buoyancy of a particle F becomes less or equal to zero.

2.5 Deposition and radioactive decay

The dry deposition flux is calculated by the following relation:

$$F_d(x,y) = V_d\, c(x,y,z=1m)$$

where V_d is the dry deposition velocity which is provided by the appropriate RODOS modules and is a function of land cover and species.

The wet deposition at a location (x,y) is calculated for each puff p with coordinates (x_p,y_p) and load Q_p from the following relation:

$$F_w(x,y) = \frac{\Lambda Q_p}{2\pi U \sigma_{xp}\sigma_{yp}}\left\{ \exp\left[-\frac{1}{2}\frac{\left(x_p - x\right)^2}{\sigma_{xp}^2} - \frac{1}{2}\frac{\left(y_p - y\right)^2}{\sigma_{yp}^2}\right]\right\}$$

where Λ (1/s) is a wet deposition coefficient, calculated as a function of the precipitation intensity I as follows:

$$\Lambda = \alpha I^{\beta}$$

The coefficients α and β are provided by the RODOS database as function of species type.

The decay of radioactive pollutants is calculated by the exponential law, using decay coefficients λ for each radionuclide, provided by the RODOS database.

Taking into account dry and wet deposition and decay of radioactive pollutants the decrease of puffs load is given by the following relation:

$$Q(t+\Delta t) = Q(t)\exp\left[-\left(\frac{2}{\pi}\right)^{1/2} \int_t^{t+\Delta t} \frac{V_d}{\sigma_z^2 \exp\left(H^2/2\sigma_z^2\right)} dt - \lambda\,\Delta t - \Lambda\,\Delta t\right]$$

3 The gamma radiation dose model description

3.1 From deposited material on the ground

For calculating the gamma radiation dose rate from radionuclides deposited on the ground the "infinite plane" assumption is adopted. This is justified by the large surface of RODOS grid cells in comparison to the height of 1 m above ground, where the dose rate is calculated. Therefore the total deposition for each radionuclide is returned by RODOS-DIPCOT to the RODOS-DOSE module. The latter calculates then the gamma radiation dose rate by multiplying the deposition with appropriate factors depending on the nuclide and organ.

3.2 From cloud

To take into account—in a computationally efficient way—the fact that more than one photon with different energies are emitted per radioactive disintegration, the energy spectrum is divided in 4 parts (Thykier-Nielsen et al., 1995) and the photons are grouped according to their energy. The groups with their nominal energies and the energy ranges are given in Table 1.

Table 1: Photon groups, nominal energies and energy ranges

Group	$E_{\gamma,nom}$ (MeV)	Energy range (MeV)
1	0.2	≤ 0.35
2	0.5	> 0.35 … 0.75
3	1.0	> 0.75 … 1.5
4	2.0	> 1.5

The energy emitted per disintegration in each of the 4 groups for each radionuclide $E_{\gamma,ig,nu}$ (*ig* = 1–4, *nu* = index for radionuclide) is read by RODOS-DIPCOT from a file in the RODOS database.

The number of "equivalent photons" $f_{ig,nu}$ emitted per disintegration in each group *ig* (i.e., with energy equal to the nominal energy of each group) for the radionuclide *nu* is calculated as follows:

$$f_{ig,nu} = \frac{E_{\gamma,ig,nu}}{E_{\gamma,\mathrm{nom},ig}}$$

To calculate the gamma radiation dose rate in air we take into account that in RODOS-DIPCOT the radioactive cloud is constituted of puffs and each puff contains all the released nuclides. So the gamma radiation dose rate at the location (x_0,y_0,z_0) (in RODOS-DIPCOT z_0 = 1 m) is calculated as the sum over all puffs, all radionuclides and the 4 energy groups, as follows:

$$\dot{D}_\gamma(x_0,y_0,z_0) = \sum_{n=1}^{N_p}\sum_{nu=1}^{N_{nucl}}\sum_{ig=1}^{4} f_{ig,nu}\frac{\mu_{\alpha,ig}E_{\gamma,ig,nu}}{\rho}\Phi_{n,nu,ig} \qquad (7)$$

where N_p is the total number of puffs, N_{nucl} the total number of radionuclides, $\mu_{\alpha,ig}$ is the total linear energy absorption coefficient for air (m^{-1}), for the energy group *ig*, ρ is the air

density (kg·m^{-3}) and $\Phi_{n,nu,ig}$ is the fluence rate (photons·m^{-2}·s^{-1}) originating from the energy group *ig* of nuclide *nu* contained in puff *n*.

Formally the fluence rate due to a radioactive cloud with concentration distribution $c(x,y,z)$ is given by the following relation:

$$\Phi(x_0,y_0,z_0)=\frac{1}{4\pi}\int_{-\infty}^{\infty}\int_{-\infty}^{\infty}\int_{-\infty}^{\infty}\frac{Be^{-\mu r}c(x,y,z)}{r^2}dxdydz \tag{8}$$

In (8) μ is the total linear attenuation coefficient for air (m^{-1}), which is a function of the photons' energy, B is the "build-up" factor, that accounts for the flux of extra photons due to Compton scattering and r is the distance between the receptor point and the elementary source of volume $dxdydz$ around the point (x,y,z), $r^2=(x-x_0)^2+(y-y_0)^2+(z-z_0)^2$. The build-up factor is calculated as $B=1+\kappa\mu r$, where $\kappa=(\mu-\mu_\alpha)/\mu_\alpha$.

The volume integral in equation (8) is computationally very expensive, if one takes also into account the large number of nuclides treated in RODOS-DIPCOT application. Therefore a method has been developed to simplify the integral (8), which is based on the work of Gorshkov et al. (1995) extended for application in a Lagrangian puff dispersion model.

The basic steps of the methodology are the following:

1. The build-up factor is expressed as differential operator.
2. For each puff a transfer and turn of the coordinates system axes is performed in such a way that the origin coincides with the centre of the puff (x_p,y_p,z_p) and the z-axis passes through the receptor point (x_0,y_0,z_0). The new sigmas are calculated for each puff in the new coordinates systems.
3. Appropriate integral representations of exponential functions, separations of variables and finally transformations of variables reduce the triple integral of (8) to a sum of integrals of 1 variable.

As a result of the above manipulations, the fluence rate entering equation (7) is written as follows:

$$\Phi_{n,nu,ig}=\frac{1}{4\pi}\frac{Q_{n,nu}}{\sigma'_{x,n}\sigma'_{y,n}\sigma'_{z,n}}\frac{1}{\mu_{ig}}\left(A_{1,n,ig}+\kappa_{ig}\,A_{2,n,ig}\right) \tag{9}$$

where $Q_{n,nu}$ is the load of puff *n* related to nuclide *nu*, $\sigma'_{x,n}$, $\sigma'_{y,n}$, $\sigma'_{z,n}$ are the sigma parameters of puff *n* in the transferred and turned coordinate system, μ_{ig} is the total linear attenuation coefficient in air for the energy group ig, and $A_{1,n,ig}$, $A_{2,n,ig}$ are the 1-variable integrals:

$$A_1=\mu h\int_0^{\infty}2\omega\,\mathrm{erfc}\left(\frac{\mu h}{2\omega}\right)\frac{1}{\sqrt{(h/\sigma_{x'})^2+2\omega^2}}\frac{1}{\sqrt{(h/\sigma_{y'})^2+2\omega^2}}\frac{1}{\sqrt{(h/\sigma_{z'})^2+2\omega^2}} \tag{9a}$$
$$\exp\left[-\omega^2/\left(1+2\omega^2/(h/\sigma_{z'})^2\right)\right]d\omega$$

$$A_2=(\mu h)^2\int_0^{\infty}\mathrm{erfp}\left(\frac{\mu h}{2\omega}\right)\frac{1}{\sqrt{(h/\sigma_{x'})^2+2\omega^2}}\frac{1}{\sqrt{(h/\sigma_{y'})^2+2\omega^2}}\frac{1}{\sqrt{(h/\sigma_{z'})^2+2\omega^2}} \tag{9b}$$
$$\exp\left[-\omega^2/\left(1+2\omega^2/(h/\sigma_{z'})^2\right)\right]d\omega$$

In (9a,b) h is the distance between the centre of the puff and point where the fluence rate is calculated.

Integrals (9a,b), although 1-dimensional, are still expensive to calculate, especially in the frame of a Lagrangian dispersion model that uses a large number of puffs (in the order of 10^3 to 10^5). The fluence rate has to be calculated at each grid point for all the puffs present in the computational domain.

To overcome this difficulty, the integrals A_1 and A_2 (9a,b) have been pre-calculated for a range of values of the parameters μh, h/σ'_x, h/σ'_y h/σ'_z. The number of values for each of the parameters is 26. Starting values are as follows: for μh 10^{-4}, next 10^{-3}, for h/σ'_x, h/σ'_y, h/σ'_z 10^{-3}, next 10^{-2}. Subsequently the steps for calculating the next values increase by a factor of 1.4 for μh and 1.5 for h/σ'_x, h/σ'_y, h/σ'_z. The maximum values are: for μh 10.12, for h/σ'_x, h/σ'_y, h/σ'_z 454.5. The above values have been selected as a compromise between the total number of values calculated for A_1 and A_2, and the range of values encountered in dispersion calculations for the different photons energies, puffs dimensions and distances between puffs and receptor (grid) points.

The pre-calculated values of the integrals have been stored in an ASCII file in the form of 4-dimensional matrices and they are read at the beginning of a DIPCOT run (arrays `DOSAR1(0:25,0:25,0:25,0:25)` and `DOSAR2(0:25,0:25,0:25,0:25)`). The values of the parameters μh, h/σ'_x, h/σ'_y h/σ'_z are also pre-stored and read at the beginning of a DIPCOT run (arrays `MAR(0:25)`, `XAR(0:25)`, `YAR(0:25)`, `ZAR(0:25)`). Each time a fluence rate has to be calculated by relation (18), a linear interpolation is performed in the values of `DOSAR1` and `DOSAR2` for the specific values of μh, h/σ'_x, h/σ'_y h/σ'_z. This is a very fast calculation saving a lot of computational time.

4 Model evaluation

4.1 Introduction

This section presents the results of a validation study of the atmospheric dispersion model DIPCOT, implemented in the RODOS system, against data from two field experiments of the Model Validation Kid (Olesen 1995; 1997). The code is tested against data involving the release of a passive tracer (SF6) from elevated point sources over a flat area in the area of Indianapolis (USA) and a suburban area in Copenhagen (Denmark).

Data from the measurements of near ground concentrations were compared with the predicted ones statistically, using appropriate performance indices, and qualitatively, using various types of plots.

4.2 Indianapolis case

4.2.1 Experimental data set

The Indianapolis field experiment (Hanna and Chang, 1993) was carried out to study the effects of SF6 releases from the Perry K Power Plant in the flat area of Indianapolis, Indiana, USA. The underlying terrain was urban with an assumed roughness length of 1 m. There were 170 hours of experimental data available, distributed at 19 sets of 8-9 hours. Approximately 4.5 to 5 g/s SF6 were released from a stack of 83.8 m height and 4.72 m in diameter, at 200 to 230 °C, with an exit velocity range of 6.5 to 15.5 m/s. The average hourly concentrations were measured from a network of ground monitors (~160), placed on 12 arcs at a distance ranging from 0.25 to 12 km. Meteorological observations were available from monitors on three towers of 10 m height each, on the top of a building at 94 m and at the local airport. There were also measurements from minisondes and acoustic sounders.

From the 19 data sets, which are available, we made use of 9 sets (covering 80 hours of simulations) representative of all the stability categories (sets 1-2-8-9-10-13-15-17 & 18). Experimental meteorological data were pre-processed by the FILMAKER diagnostic meteorological code to obtain the required for atmospheric dispersion calculations meteorological. The computational domain covers 14 km around the source. The horizontal discretisation was 16×23 cells raging from 1×1 km^2 (near the source) up 2.5 × 2.5 km^2 at the edges. The vertical discretisation consisted of 23 cells with dimensions varying from 10 to 500 m, extending up to 4 km in height.

Hourly or (when available) half-hourly data from the meteorological observations have been used by the pre-processor to calculate by interpolation the required 2 and 3-dimensional fields for the dispersion model (mean wind velocity, temperature, pressure, mixing layer height, friction and convective velocity, atmospheric stability and Monin-Obukhov length etc).

Atmospheric dispersion calculations were performed by DIPCOT using a release rate of 1 particle/sec. The mean ensemble concentration of the pollutant, at each receptor of the arcs, was obtained, from the spatial and temporal distribution of the particles, using the kernel density estimator of Yamada and Bunker (1988), every 10min. The mean hourly ground average concentrations were easily estimated, in order to perform comparisons with the experimental data.

4.2.2 Evaluation procedure

The most common evaluation procedure is to compare the predicted concentrations with the observed ones. In this case study we used the arc-wise maximum method (Olesen, 1995), which deals only with the maximum concentrations along each monitoring arc. The maximum observed concentrations at each arc were compared with the estimated maximum concentrations at the same arc, no matter where on the arc they occur.

The evaluation of the model has been performed comparing the predicted concentrations with the observed ones using well-known statistical indices [e.g. Hanna, 1989 and Mosca et al., 1994] such as: the Fractional Bias: $FB = 2(\overline{C_o} - \overline{C_p})/(\overline{C_o} + \overline{C_p})$, where C_o and C_p are the observed and the calculated concentration respectively, the Geometric Mean bias: $MG = \exp\left[\overline{\ln(C_o / C_p)}\right]$, the Normalised Mean Square Error: $NMSE = \overline{(C_o - C_p)^2} / \overline{C_o}\,\overline{C_p}$, Geometric mean Variance: $VG = \exp\left[\overline{\ln(C_o / C_p)^2}\right]$, the *FACT*or of x (x = 2, 5 and 10), which is the fraction of the C_p that falls within C_o/x and x·C_o, and the Factor Of Exceedance: $FOEX = (N_{Cp>Co} / N - 0.5) \times 100$ where $N_{Cp>Co}$ is the number of overpredictions, and N the total number of pairs used for the comparisons.

The statistic measures *FB* and *NMSE* give more weight to large values of C_o and C_p, while *MG* and *VG* give equal weight to all pairs. A "perfect" model exhibits zero value for both *FB* and *NMSE* and unit value for *MG* and *VG*. Values of *FB* less than zero and *MG* less than one mean that the model overpredicts. Moreover, if the confidence limits of *FB* overlap *FB* = 0 then the calculated *FB* is not significantly different from zero at the 95% confidence level. The *NMSE* and *VG* values give information on the deviations and not on the over- and under-prediction and thus are always positive. If a model has very law *NMSE* means that it performs well in space and time. However, models that present higher values of *NMSE* do not necessarily have a poor performance. Differences on peak values between the predicted and the observed concentrations have a higher influence on the value of *NMSE*. Contrary to the *NMSE*, *VG* gives the same weight to all values, showing the same ratio independently from the absolute value of the data. The *FOEX* ranges between –50% and +50%; the best value is 0%, which means that the over-predictions equal the under-predictions. Less than zero values denote under-prediction. The *FOEX* values must be used in conjunction with the *FACTx* values. The index *FACTx* (*FACT*2, *FACT*5 & *FACT*10) takes values between 0 and 100%. The higher values of *FACTx* indicate good overall agreement with observations, especially as the index *FACT*2 converge to 100.

All the above indices were estimated by the METeorological and DISpersion STATistics code (Deligiannis et al., 1997). The 95% confidence interval limits for *FB* and *MG* were also estimated, based on the Bootstrap re-sampling method (Hanna, 1989). It consists in re-sampling for a number of times (1000 in this case) the set of pairs, with possible repetitions of pairs, and each time re-estimate the statistical indices. From the distribution of these values, the values corresponding to 2.5% and 97.5% cumulative probability are taken as the limits of the confidence interval.

In addition to the statistical approach, the model's behaviour is also examined qualitatively, through the scatter plot of the corresponding maximum arc-wise observed and predicted concentrations and the quantile-quantile (Q-Q) plot of the ranked observed and predicted values, which give a quick view of the model behaviour.

4.2.3 Results

The comparison between the arc-wise maximum concentrations using the statistical indices is presented in Fig 1 and 2. The values of the performance indices are within acceptable ranges that are characteristic of those found for other models dispersion models applied to various data sets (Hanna, 1989). More than 42% of the maximum arc-wise predicted concentrations falls close to the observed ones (*FACT*2 ~ 42%). Moreover, the vast majority of the predictions are within acceptable range, as indicated by the values of *FACT*5 and *FACT*10, which are close to 77% and 87%, and the values of *FB*, *MG* that are close to 0, 1 respectively.

The model has a slight tendency to overestimate the observed values. This is indicated by the negative value of *FB* (-0.172), that denotes 17.2% over-prediction of the mean of the estimated values for all hours over the mean of the observed values for all hours, and the lower than unit value of MG. However, the model does not exhibit a systematic tendency towards over-predictions since the confidence limits for both indices include zero and unit. This can also be observed from the value of the *FOEX* index (which is relatively close to zero) and the scatter plot.

The relatively higher value of VG indicates greater deviations in the smaller concentrations, while the close to zero value of *NMSE* displays a less scatter from the observed data over the higher concentrations, which can also be observed in the scatter and the Q-Q plot. From the Q-Q plot it is obvious that the model predictions, even though they present deviations from the observed concentrations, approximate in an acceptable way the range of the observed maximum concentrations.

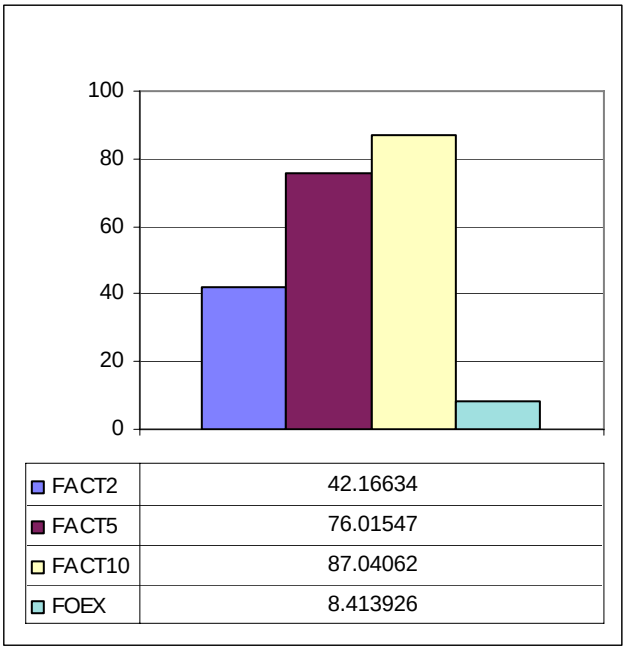

Figure 1: Values of *FACT*x and *FOEX*.

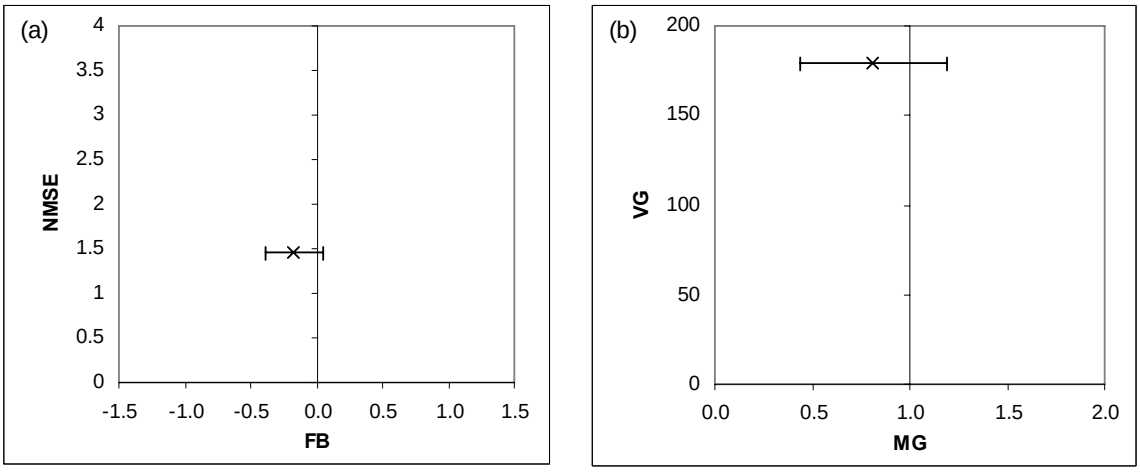

Figure 2: Values of *FB* and *MG* (with their 95% confidence interval limits) vs *NMSE* and *VG*.

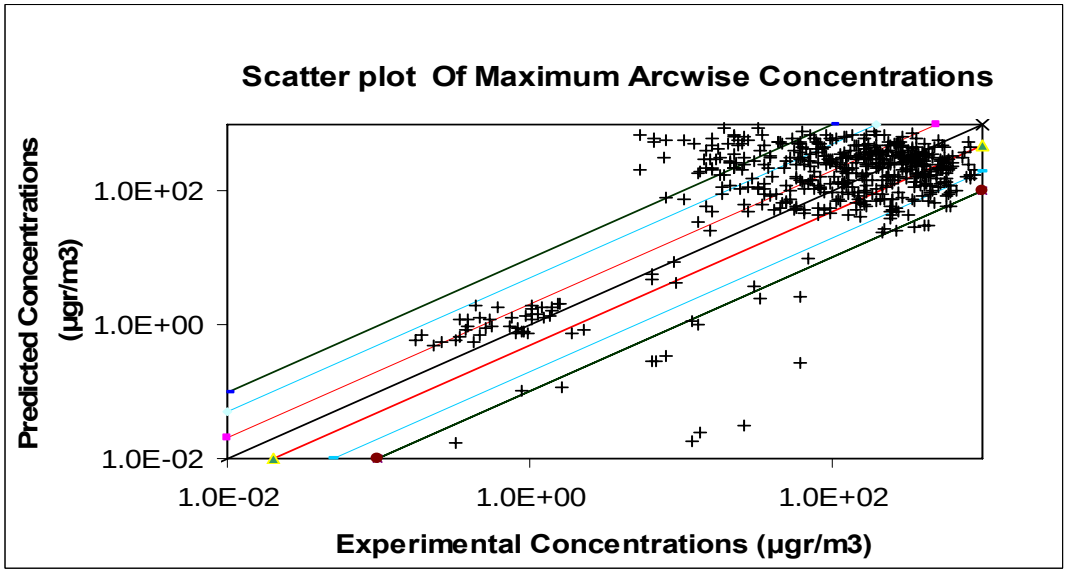

Figure 3: Scatter plot of experimental vs modelled arc-wise maximum concentrations

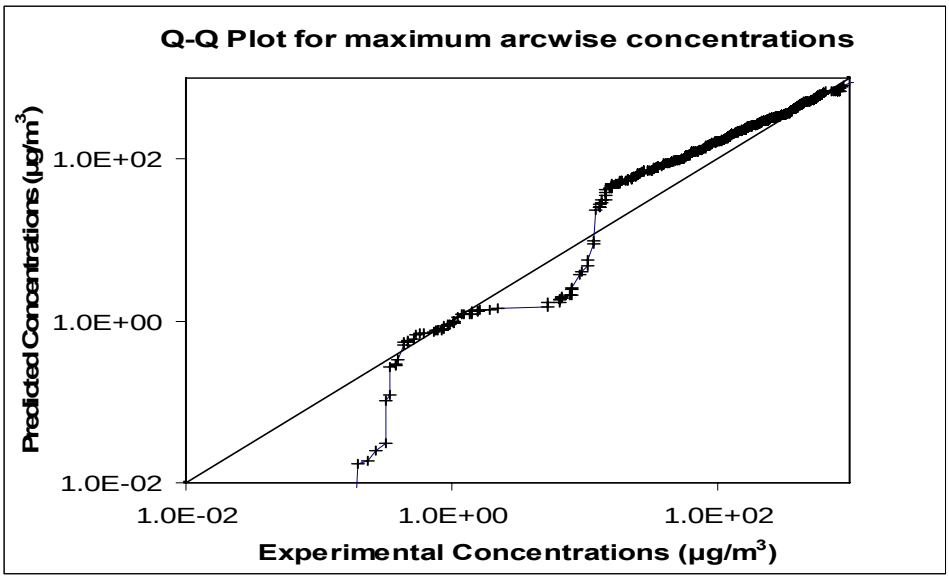

Figure 4: Q-Q plot of experimental vs modelled arc-wise maximum concentrations

4.3 The Copenhagen case

4.3.1 Experimental data set

Gryning and Lyck conducted a field study in a suburban area in Copenhagen during 1978 and 1979, to examine dispersion of elevated sources in urban areas (Gryning 1981, Gryning and Lyck 1984). SF6 (sulphur hexafluoride) was released from a 115 m high tower, and sampled at receptors laid out in three arcs at distances of 2, 4, and 6 km from the release point. Typically 20 tracer sampling units were used in each arc, as presented in Figure 5.

The concentrations were measured near ground, at 2–3m height, and averaged over 20 min. The experiment resulted in about 10 h of data collected during neutral and unstable atmospheric conditions (3 experiments under neutral conditions and 7 under slightly unstable and unstable). The pollutant was released at steady rate in each experiment (at a rate from 2.3gr/s to 4.7 gr/s) at air temperature.

The site was mainly residential having a roughness length of 0.6 m. The meteorological measurements performed during the experiments included standard measurements along the tower of tracer release as well as the three-dimensional wind velocity fluctuations at the height of release. The meteorological measurements were pre-processed by the FILMAKER diagnostic meteorological code.

Atmospheric dispersion calculations were performed by RODOS-DIPCOT using a release rate of 1 particle/sec. The concentration at each receptor was estimated using, as in the Indianapolis case, the kernel density estimator of Yamada and Bunker (1988) at time steps of 1 min, which are then averaged in order to obtain mean steady-state concentrations.

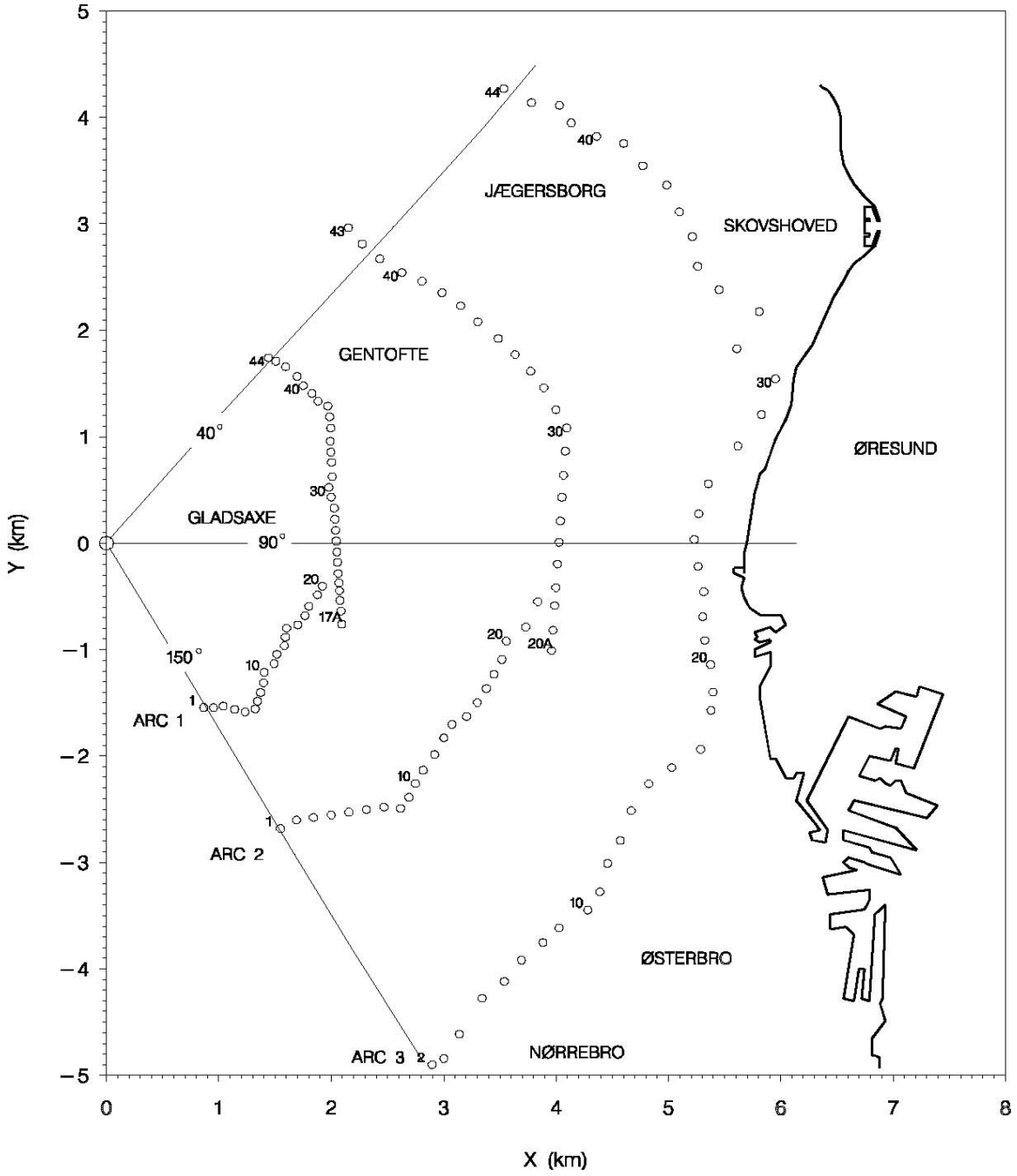

Figure 5: The area for the tracer experiments.

4.3.2 Evaluation procedure

In this case study we used the arc-wise maximum method, as described in the Indianapolis case. Moreover, for all runs during the experiment, from the crosswind profiles of tracer concentrations determined along each arc, the crosswind integrated concentrations C_Y and the lateral standard deviation of the tracer concentration distribution *SIGY* (Gryning, 1981). The comparisons between the experimental and the estimated values were made using the statistical indices, described in the Indianapolis case and scatter plots.

4.3.3 Results

The statistical comparison between the arcwise maximum concentrations (*ARCMAX*), the crosswind integrated concentrations (*CY*) and the lateral standard deviation of the tracer concentration distribution (*SIGY*) are presented in Table 1.

Table 1: Statistical indices for the Copenhagen Experiment (FB with its 95% confidence interval limits, *NMSE*, *FACT*2, *FACT*5 and *FOEX*) for *ARCMAX*, *CY* and *SIGY*

	ARCMAX	***CY***	***SIGY***
FB	0.71	0.16	-0.02
(*FB*-, *FB*+)	(0.62,0.79)	(0.08, 0.25)	(-0.10, 0.06)
NMSE	0.93	0.09	0.07
***FACT*2–*FACT*5**	43. – 100.	100.-100.	100.-100.
FOEX	-45.65	-28.26	0.

The model gives better performance in estimating integrated concentration rather than maximum concentration. This is obvious from almost all the statistical indices. The deviations between the observed and modelled data are smaller for the *CY* concentrations (larger *FACT*2, smaller *FB* and *NMSE* values). The model for both *ARCMAX* and *CY* predictions lead to a positive bias ($FB > 0$, $FOEX < 0$), i.e. to general underestimation of the concentration data. However, this tendency is clearer to the estimation of the maximum concentrations. This can be observed in the scatter plots at Figures 6 and 7, and it is verified by the difference between the values of *FB* for the *ARCMAX* and *CY* concentrations.

The model exhibits a tendency to overestimate the lateral crosswind spread (*SIGY*) of the plume ($FB < 0$). However, this trend can be characterized as a slight one and not systematically. This is indicated by the fact *FB* is almost zero, the 95% confidence interval limits of FB include the zero value and the value of *FOEX* is relatively close to zero (see also Figure 8)

The overall performance of the model can be considered as satisfactory. Once again, as in the Indianapolis case, more than 40% of the maximum arc-wise predicted concentrations falls close to the observed ones (*FACT*2 ~ 44%) and the vast majority of all the predictions are do not present large scatter (*FACT*5 ~ 100%, *NMSE* ~ 1). The corresponding values for the *CY* and *SIGY* are quite improved in regard to *ARCMAX*. The *FACT*2 index (for both *CY* and *SIGY*) and the values of *FB*, *NMSE* and *FOEX* (for *SIGY*) approximate the values of a "perfect" dispersion model, indicating much better agreement with the measurements. The performance of DIPCOT is comparable to other models that have been evaluated using the Copenhagen data set (e.g., see Vitali et al., 2006).

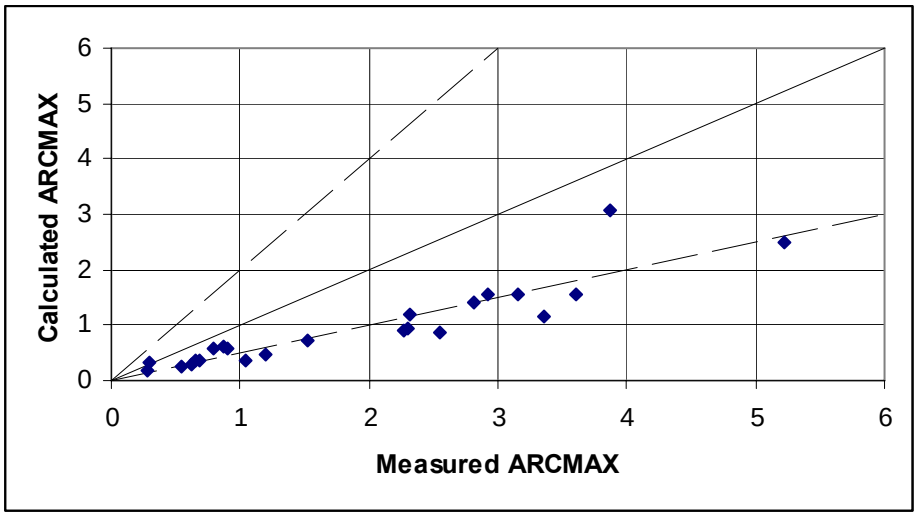

Figure 6: Scatter plot of experimental vs modelled arcwise maximum concentrations

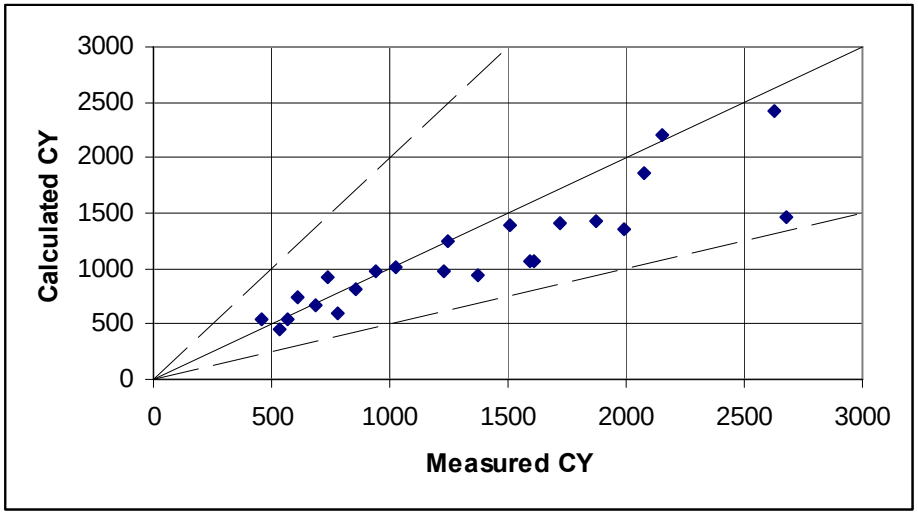

Figure 7: Scatter plot of experimental vs modelled crosswind integrated concentrations

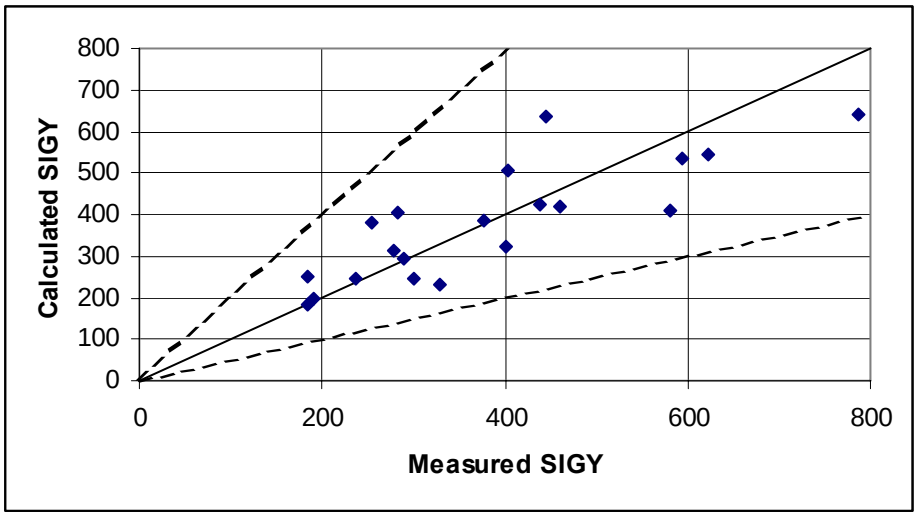

Figure 8: Scatter plot of experimental vs modelled lateral standard deviation of the tracer concentration distribution (*SIGY*)

4.4 Conclusions

The performance of Lagrangian particle dispersion model RODOS-DIPCOT was evaluated against two well known field experiments of the Model Validation Kid: the Copenhagen and the Indianapolis case. The selected cases cover all the atmospheric stability conditions. The model predictions were statistically and qualitatively compared with the observed ones through indices and methods widely used in the literature. The results showed that in all cases the model simulates with acceptable accuracy atmospheric dispersion in levels that are comparable to other models.

5 References

Baerentsen, J.H., and R. Berkowicz, 1984: 'Monte Carlo simulation of plume dispersion in the convective boundary layer', *Atmospheric Environment* 18, 701-712.

Borgas, M.S. and B.L. Sawford, 1994: 'A family of stochastic models for two-particle dispersion in isotropic homogeneous stationary turbulence', *J. Fluid Mech*., vol. 279, pp. 69-99

Davakis E., Nychas, S.G., Andronopoulos, S. and Bartzis, J.G., 2003: 'Validation study of the Lagrangian dispersion particle model DIPCOT over complex topographies using different concentration calculation', Int. J. Environment and Pollution, 20, Nos 1-6, 33-46

Deligiannis, P., J.G., Bartzis, E., Davakis, (1997), 'Complex terrain modelling exercise', Int. J. Environment and Pollution, Vol. 8 Nos. 3-6, pp 367-377

Gryning, S., 1981: Elevated Source SF6-Tracer Dispersion Experiments in the Copenhagen Area. Report Risø-R-446, Risø National Laboratory, DK-4000 Roskilde, Denmark

Gryning, S. and Lyck, E., 1984: Atmospheric dispersion from elevated sources in an urban area: comparison between tracer experiments and model calculations. *Journal of Climate & Applied Meteorology* **23**, pp. 651–660

Gorshkov V.E., I.P. Karmazin, and V.I. Tarasov (1995) "Reduced Integral Solutions for Gamma Absorbed Dose from Gaussian Plume", Health Phys. 69(2), pp. 210-218

Gryning, S.E., A.A.M., Holstag, J.S., Irwin, and B., Sivertsen, (1987), "Applied dispersion modelling based on meteorological scaling parameters., *Atmospheric Environment*, **21**, 79–89.

Hanna, S.R., (1982), 'Atmospheric turbulence and air pollution modeling', F.M.T. Nieuwstadt, and H. van Dop, Editors, Dordrecht, Holland: D. Reidel, 275–310

Hanna, S.R., 1989: Confidence limits for air quality models, as estimated by bootstrap and jack-knife resampling methods, *Atmospheric Environment*, **23**, No. 6, pp. 1385-1395

Hanna, S.R., and R.J., Paine, 1989: 'Hybrid plume dispersion model (HPDM) development and evaluation', *J. of Applied Meteorology*, **28**, pp 206-224

Hanna S.R. & Chang J.C., 1993: Hybrid plume dispersion model (HPDM) Improvements and testing at three field sites, *Atmospheric Environment*, **27A**, No. 9, p. 2265 – 2285

Holtslag, A.A.M., and C. H., Moeng, (1991) 'Eddy diffusivity and countergradient transport in the convective atmospheric boundary layer', *J. of Atmos. Science*, **48**, 1690–1998.

Hurley P., and W. Physick, 1993: 'A skewed homogeneous Lagrangian particle model for convective conditions', *Atmospheric Environment*, **27A**, No. 4, pp. 619-624.

Monin A.S. and Yaglom M.A., 1975: 'Statistical Fluid Mechanics', Vol. 2, MIT Press, Cambridge, Massachusetts, 875.

Luhar, A.K. R.E. Britter, 1989: 'A random walk model for dispersion in inhomogeneous turbulence in a convective boundary layer', *Atmospheric Environment*, **23**, No 9, pp. 1911-1924.

Luhar, A.K. and W.H. Rao, 1993: 'Random walk model studies of the transport and diffusion of pollutants in katabatic flows', *Boundary Layer Meteorology*, **66**, pp. 395-412

Mosca, S., G. Graziani, W. Klug, R. Roberto, R. Bianconi, 1998: A statistical methodology for the evaluation of long – range dispersion models: An application to the ETEX exercise. *Atmospheric Environment*, **24**, 4307-4324

Olesen, H.R., 1995: 'Dataset and protocol for model validation' Kit', *Int. J. Environment and Pollution*, **5**, Nos. 4-6, pp 693-701

Olesen H.R., 1997: Pilot study: extension of the Model Validation Kit, *Int. J. Environment and Pollution*, **8**, Nos. 3 - 6, p. 378 - 387

Taylor, G.I., 1921: 'Diffusion by continuous movements', Proceedings, London Math., **20**, 169-211.

Thomson D.J., 1987: 'Griteria for the selection of stochastic models of particle trajectories in turbulent flows', *Journal of Fluid Mechanics*, **180**, pp. 529-556

Thykier-Nielsen S., Deme S. and Lang, E., 1995: 'Calculation method for Gamma dose rates from Gaussian puffs'. Report Risø-R-775(EN), Risø National Laboratory, Roskilde, Denmark.

Thykier-Nielsen S., Deme S. and Mikkelsen T., 1998: "Description of the Atmospheric Dispersion Module RIMPUFF". Report RODOS(WG2)-TN(98)-02.

Uliasz, M., 1994: Lagrangian particle dispersion modelling in mesoscale applications. Environmental Modelling II, Computational Mechanics Publications, P. Zanneti (Editor), 71-102

Vitali, L., Monforti, F., Bellasio, R., Bianconi, R., Sachero, V., Mosca, S., Zanini, G., 2006: Validation of a Lagrangian dispersion model implementing different kernel methods for density reconstruction, *Atmospheric Environment*, **40**, 8020–8033

Weil J.C., 1990: 'A diagnosis of the asymmetry in top-down and bottom-up diffusion using a Lagrangian stochastic model', *J. of Atmospheric Sience*, **47**, pp 501-515

Wilson J.D. and B.L. Sawford, 1996: 'Review of Lagrangian Stohastic Models for Trajectories in the Turbulent Atmosphere', *Boundary Layer Meteorology* **78**, pp. 191-210

Yamada T. and Bunker S., (1988): 'Development of a nested grid, second moment turbulence closure model and application to the 1982 ASCOT Brush Creek data simulation', *Journal of Applied meteorology,* **27**, 562–578.

6 Document History

Document Title:	RODOS-DIPCOT Model Description and Evaluation
EURANOS number:	RODOS(RA2)-TN(09)-01
Version and status:	Version 1.0 (final)
Issued by:	S. Andronopoulos
History:	
Date of Issue:	31 July 2009
Circulation:	
File Name:	RA2TN0901_DIPCOT
Date of print:	05 August 2009